Available online at www.sciencedirect.com
ScienceDirect
Polymer 48 (2007) 997–1004
polymer
www.elsevier.com/locate/polymer

Microphase-separated structure and mechanical properties of norbornane diisocyanate-based polyurethanes

Ken Kojio [a], Shohei Nakashima [b], Mutsuhisa Furukawa [b,*]

[a] *Department of Materials Science and Engineering, Faculty of Engineering, Graduate School of Science and Technology, Nagasaki University, 1-14 Bunkyo-machi, Nagasaki 852-8521, Japan*
[b] *Department of Materials Science, Graduate School of Science and Technology, Nagasaki University, 1-14 Bunkyo-machi, Nagasaki 852-8521, Japan*

Received 20 June 2006; received in revised form 8 December 2006; accepted 28 December 2006
Available online 7 January 2007

Abstract

Norbornane diisocyanate (NBDI: 2,5(2,6)-bis(isocyanatomethyl)bicyclo[2.2.1]heptane) is a new commercialized diisocyanate. NBDI-based polyurethane elastomers (PUEs) were prepared from poly(oxytetramethylene) glycol (PTMG), NBDI and 1,4-butanediol (BD) by a prepolymer method. Microphase-separated structure and mechanical properties of the NBDI-based PUEs were compared with general aliphatic and cycloaliphatic diisocyanate-based PUEs. The diisocyanates used were isophorone diisocyanate (IPDI), 4,4′-dicyclohexylmethane diisocyanate (HMDI) and 1,6-hexamethylene diisocyanate (HDI). Regular polyurethanes were also prepared as hard segment models from each isocyanate and BD to understand the feature of each hard segment chain. The HDI-based PUE showed the largest Young's modulus and tensile strength in the four PUEs due to the ability of crystallization of the hard segment component and the strongest microphase separation. HMDI has both properties of aliphatic and cycloaliphatic diisocyanates because of its high symmetrical chemical structure compared with NBDI and IPDI. On the other hand, the NBDI- and IPDI-based PUEs have an inclination to phase mixing, leading to decreased Young's modulus and tensile strength. The NBDI-based PUE exhibited better thermal properties at high temperatures due to stiff structure of NBDI.

Keywords: Norbornane diisocyanate; Cycloaliphatic diisocyanate; Polyurethanes

1. Introduction

Polyurethanes (PUs) are widely used as sealant, adhesives, fibers and so on. Characteristic properties of the PUs depend on chemical structure and superstructure originated from hydrogen bond and microphase-separated structure. Namely, the hard segment domains in the PU elastomers (PUEs) can act as crosslinking points like reinforced filler, but they sometimes make difficult to control the mechanical properties precisely [1–10]. The superstructure of the PUEs strongly depends on the molecular weight of soft segment, hard segment content, preparation conditions, and chemical structure of raw materials. Diisocyanates can be classified into aromatic and aliphatic diisocyanates. Aromatic diisocyanate-based PUEs generally bear the superior mechanical properties due to strong cohesion force between the hard segment chains. However, the aromatic diisocyanate-based PUEs possess the serious defects' properties such as the change of color against ultraviolet and visible light and heat [11–13]. In contrast, the aliphatic diisocyanate-based PUEs do not show the change of color under same condition.

2,5(2,6)-Bis(isocyanatomethyl)bicyclo[2.2.1]heptane (norbornane diisocyanate: NBDI) was recently developed as a novel diisocyanate [14]. Norbornane is a bicyclic alkane containing a bridged six-member ring. Since norbornane derivatives generally possess a high transparency [15], damping [16] and filtration properties, they are applied to photo-resist materials, waveguides, insulators, filtration membranes, shape memory materials and so on. Thus, it is expected that NBDI would show good mechanical and thermal properties for the

* Corresponding author. Tel.: +81 95 819 2650; fax: +81 95 819 2651.
E-mail address: furukawa@nagasaki-u.ac.jp (M. Furukawa).

0032-3861/$ - see front matter © 2007 Elsevier Ltd. All rights reserved.
doi:10.1016/j.polymer.2006.12.057

incorporation as a component of the PUEs. Inoue et al. [17] reported that the NBDI-based PUE possesses low glass transition temperature and high temperature stability from measurement of the temperature dependence of dynamic mechanical properties. However, there is an open-question on the relationship between the microphase-separated structure and properties of the PUEs precisely.

In this study, we investigated the microphase-separated structure and mechanical properties of the NBDI-based PUEs by Fourier transform infrared spectroscopy (FT-IR), differential scanning calorimetry (DSC), dynamic viscoelastic properties, and compared the NBDI-based PUEs with other typical aliphatic diisocyanate-based PUEs.

2. Experimental

Poly(oxytetramethylene) glycol (PTMG: $M_n = 2000$, Nippon Polyurethane Industry Co., Ltd., Japan) was employed as a polymer glycol. The polymer glycol was dried with dried nitrogen under a reduced pressure for ca. 4 h before use. The amount of residue water was checked with Karl Fischer titration. Norbornane diisocyanate (NBDI: Mitsui Chemical, Co., Ltd., Japan), isophorone diisocyanate (IPDI: Nippon Polyurethane Industry Co., Ltd., Japan), 4,4′-dicyclohexylmethane diisocyanate (HMDI: Sumitomo Bayer Urethane Co., Ltd., Japan), and 1,6-hexamethylene diisocyanate (HDI: Nippon Polyurethane Industry Co., Ltd., Japan) were used as received. Fig. 1 shows the chemical structures of diisocyanates used in this study. The purities of the diisocyanates were confirmed to be more than 99% by an amine equivalent method. 1,4-Butanediol (BD: Wako Chemical Co., Ltd., Japan) was used as a curing agent. In order to evaluate the miscibility between the hard segment and soft segment and mechanical properties, the hard segment contents of the PUEs were changed from 10 to 50 wt%. Prepolymers were prepared from the dried polymer glycol and diisocyanate with the various ratios of $K = [NCO]/[OH]$ at 75 °C for 5 h under a nitrogen atmosphere. One drop of dibutyltin dilaurate (DBTL: Wako Chemical Co., Ltd. Japan) as a catalyst was added in later step of the prepolymer reaction. The extent of reaction of hydroxyl group with isocyanate was pursued by an amine equivalent method. After finishing the reaction, the prepolymer was placed under reduced vacuum at 70 °C to remove bubbles involved inside. The prepolymer and curing agent were mixed well with the ratio of $[NCO]_{pre}/[OH] = 1.05$ for 90 s, and the viscous product was poured into a mold constructed by a spacer of 2 mm thickness and two aluminum plates heated at 100 °C, where $[NCO]_{pre}$ is the molar number of NCO groups in the prepolymer. The PUEs were demolded after 2 h curing, and then, they were postcured at 80 °C for 48 h in air.

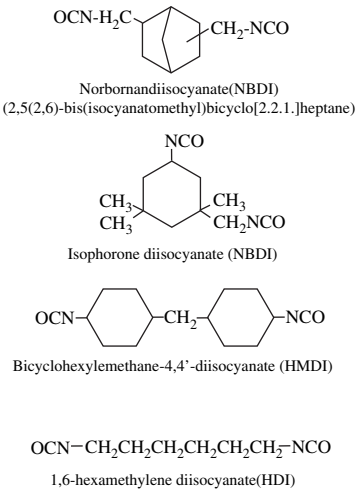

Fig. 1. Chemical structures of diisocyanates used in this study.

The regular polyurethanes as a hard segment model were synthesized by reacting each diisocyanate and BD with $K = 1.02$ at 70 °C. The hard segment model polyurethanes using NBDI, IPDI, HMDI, and HDI are referred to −(NB−BD)$_n$−, −(IP−BD)$_n$−, −(HM−BD)$_n$− and −(HD−BD)$_n$−, respectively.

The state of hydrogen bond among the hard segment chains in the PUEs was measured by attenuated total reflection Fourier transform infrared spectroscopy (ATR-FT-IR). ATR-FT-IR spectra were obtained with FTS-3000 EXCALIBUR (Digilab Japan Co., Ltd., Japan) equipped with a TGS detector using an ATR cell (MIRacle, PIKE Technologies, Inc., USA) with 32 scans and a resolution of 4 cm^{-1}.

Chain structures of the PUEs were evaluated using wide angle X-ray diffraction (WAXD). WAXD profiles were obtained with a 2θ scan mode by a RINT2200 (Rigaku Co., Ltd., Japan). Voltage and current of an X-ray source were set to 40 kV and 40 mA, respectively.

Thermal properties were analyzed by DSC. The thermograms were obtained with a DSC (Rigaku DSC 8230, Rigaku Denki Co., Ltd., Japan) from −130 to 250 °C with a heating rate of 10 °C min^{-1} under a nitrogen atmosphere. As-prepared samples were simply cooled down to around −140 °C and then the measurements were started.

The dynamic viscoelastic properties were measured with a DMS 6100 (Seiko Instruments, Co., Ltd., Japan) between −150 and 250 °C with a heating rate of 2 °C min^{-1} under a nitrogen atmosphere. The size of samples used is 25 mm × 5 mm × 2 mm. Imposed strain and frequency were 0.2% and 10 Hz, respectively.

Tensile testing was performed with an Instron type tensile tester (Shimadzu Autograph; AGS−100A, Japan) at 20 °C. The dimension of samples is 60 mm × 5 mm × 2 mm. An initial length and elongation rate were set to 15 mm and 5 mm min^{-1}, respectively.

3. Results and discussion

3.1. Chain structure of hard segment models

Figs. 2 and 3 show the DSC thermograms and WAXD profiles of the hard segment model polyurethanes, −(NB−BD)$_n$−, −(IP−BD)$_n$−, −(HM−BD)$_n$− and −(HD−BD)$_n$−. For −(NB−BD)$_n$− and −(IP−BD)$_n$−, no characteristic peaks were observed in the DSC thermograms, indicating that these

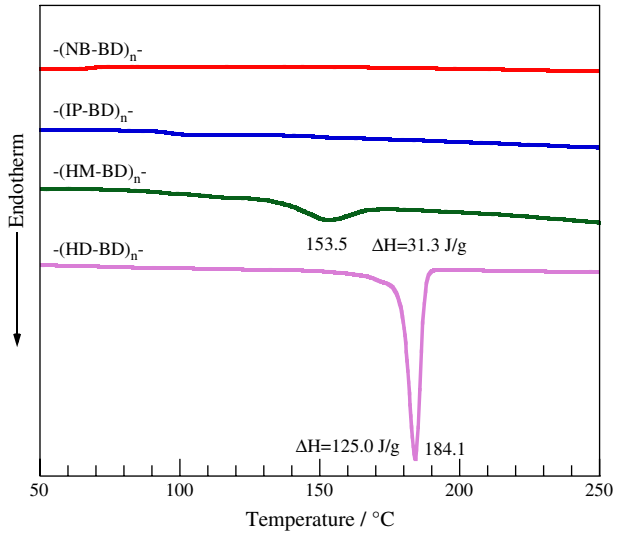

Fig. 2. DSC thermograms of hard segment models of −(NB−BD)$_n$−, −(IP−BD)$_n$−, −(HM−BD)$_n$− and −(HD−BD)$_n$−.

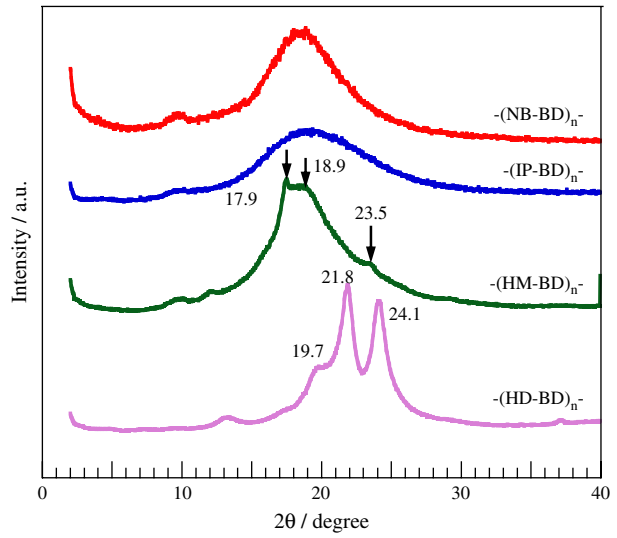

Fig. 3. WAXD profiles of hard segment models of −(NB−BD)$_n$−, −(IP−BD)$_n$−, −(HM−BD)$_n$− and −(HD−BD)$_n$−.

hard segment models are in the amorphous state. On the other hand, the DSC thermograms of −(HM−BD)$_n$− and −(HD−BD)$_n$− clearly showed endothermic peaks at 153.5 and 184.1 °C, respectively. The heat of fusion for two crystallized hard segment models were 31.3 and 125.0 J/g, respectively. WAXD profiles of −(NB−BD)$_n$− and −(IP−BD)$_n$− only exhibited amorphous halo at around 19°. On the other hand, one can see the crystalline peaks as well as amorphous halo for −(HM−BD)$_n$− and −(HD−BD)$_n$−. Crystalline peaks of −(HM−BD)$_n$− were much weaker than those of −(HD−BD)$_n$−, which is quite consistent with the results obtained by DSC. The crystal system of −(HD−BD)$_n$− is triclinic and lattice constants are $a = 0.948$ nm, $b = 0.471$ nm, $c = 1.94$ nm, $\alpha = 116°$, $\beta = 105°$, and $\gamma = 109°$ [18]. These results clearly indicate that −(NB−BD)$_n$− and −(IP−BD)$_n$− are in amorphous state, while −(HM−BD)$_n$− and −(HD−BD)$_n$− are in crystalline state at room temperature. Crystallinity of −(HD−BD)$_n$− is much higher than that of −(HM−BD)$_n$−. The fact that −(HM−BD)$_n$− is crystallizable can be attributed to its symmetrical chemical structure, although the HMDI includes some isomers.

3.2. Microphase-separated structure of polyurethane elastomers

Nomenclature of the samples denotes the type of diisocyanate and the hard segment content of the PUEs. Fig. 4 shows the ATR-FT-IR spectra of the NH stretching (ν(NH)) and C=O stretching (ν(C=O)) band region for (a) NB-, (b) IP-, (c) HM- and (d) HD-based PUEs with various hard segment contents. Generally, free NH stretching band ($\nu(NH)_{free}$), hydrogen bonded NH groups with ether oxygen ($\nu(NH)_{ether}$) and urethane carbonyl oxygen ($\nu(NH)_{carbonyl}$) are observed at 3450, 3290−3310 and 3300−3350 cm^{-1}, respectively [19,20]. On the contrary, for the C=O stretching bands (ν(C=O)), two peaks are observed at around 1687−1704 and 1730 cm^{-1}, which can be assigned to hydrogen bonded carbonyl stretching band ($\nu(C{=}O)_{H\text{-}bond}$) and free one ($\nu(C{=}O)_{free}$) [19,20]. For the NB-, IP- and HD-based PUEs with various hard segment contents, ν(NH) was only observed at around 3320 cm^{-1}. These results indicate that a number of NH groups of these PUEs form hydrogen bonds with carbonyl oxygens. For the HM-based PUE, both weak and strong peaks at 3450 and around 3320 cm^{-1} were observed above the hard segment content of 20 wt%. These results suggest that a large amount of NH groups form hydrogen bonds, but some of them do not. Also, the peak width of the NB-, IP- and HM-based PUEs was much broader than the HD-based PUE. Hence, it is likely to consider that NH groups in the NB-, IP- and HM-based PUEs form hydrogen bond with ether and carbonyl groups, but most of those in the HD-based PUE form hydrogen bonds with carbonyl oxygens.

Fig. 5 shows the hard segment content dependence of relative intensity of carbonyl groups ($I_{\nu(C=O)H\text{-}bond}/I_{\nu(C=O)free}$). For three cycloaliphatic diisocyanate-based PUEs, $I_{\nu(C=O)H\text{-}bond}/I_{\nu(C=O)free}$ gradually increased with increase in hard segment content. The increment of the relative intensity of the NB-based PUE was larger than those of other cycloaliphatic diisocyanate-based PUEs, indicating that urethane groups in the NB-based PUE aggregate stronger than for the IP- and HM-based PUEs with hydrogen bonds. On the contrary, the relative intensity of the HD-based PUE abruptly increased with increasing hard segment content and showed quite large number (∼3). Thus, it is likely to consider that the cohesion force of the hard segment chains of three cycloaliphatic diisocyanate-based PUEs is weak due to the steric hindrance of the cycloaliphatic rings. This trend was most obvious for the HM-based PUEs, which is consistent with ν(NH) in Fig. 4(c).

Fig. 6 shows the DSC thermograms of (a) NB-, (b) IP-, (c) HM- and (d) HD-based PUEs with various hard segment contents. Glass transition temperatures (T_g) of the soft segment chains were observed at around −70 °C for all PUEs. For the NB-, IP- and HM-based PUEs with hard segment content of 10 wt%,

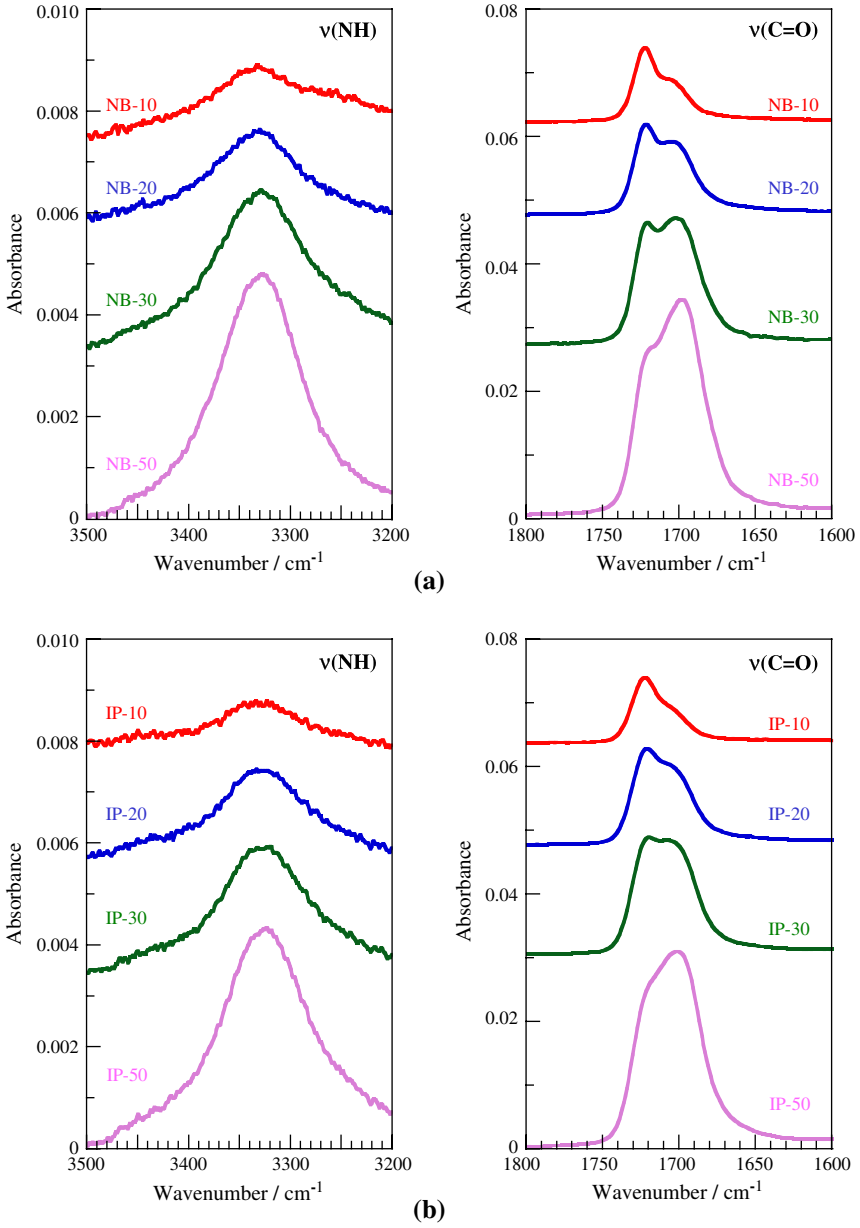

Fig. 4. ATR-FT-IR spectra of (a) NB-, (b) IP-, (c) HM- and (d) HD-based PUEs with hard segment content from 10 to 50 wt%.

strong exothermic peak due to reorganized-crystallization of the soft segment chains and endothermic peak assigned to melting of crystallized soft segment chains were observed at around −30 and 17 °C, respectively. This can be explained by the fact that the hard segment chains dispersed in soft segment matrix interrupt the crystallization of the soft segment chains during cooling process before starting DSC measurement. These exothermic and endothermic peaks disappeared with increasing hard segment content. This is simply due to the restriction of reorganized-crystallization of the soft segment chains because of a number of hard segment chains. For the HD-10 PUE, endothermic peak of melting of crystallized soft segment was observed at 18.4 °C and its peak intensity and temperature decreased with increasing hard segment content. This is also because the hard segment component dissolved into the soft segment phase restricted the crystallization of the soft segment chains. The melting peak of the hard segment domain was not observed for the NB- and IP-based PUEs with all hard segment contents, but was observed for the HM- and HD-based PUEs with a certain hard segment content. The melting of the hard segment domains for the HM-50 PUE was observed at 151.7 °C. For the HD-based PUEs, they did not show the melting of the hard segment domains at a hard segment content of 10 wt%, in contrast the melting peak temperature increased from about 120 to 167.5 °C above hard segment content of 20 wt%. Also, the heat of fusion of the hard segment domains in the HD-based PUEs increased with increasing hard segment content. These results clearly suggest that the hard segment chains were in the crystalline state for the HD- and HM-based PUEs, but not for the NB- and IP-based PUEs.

Fig. 7 shows the hard segment content dependence of T_g of the soft segment ($T_{g,s}$) for the NB-, IP-, HM- and HD-based

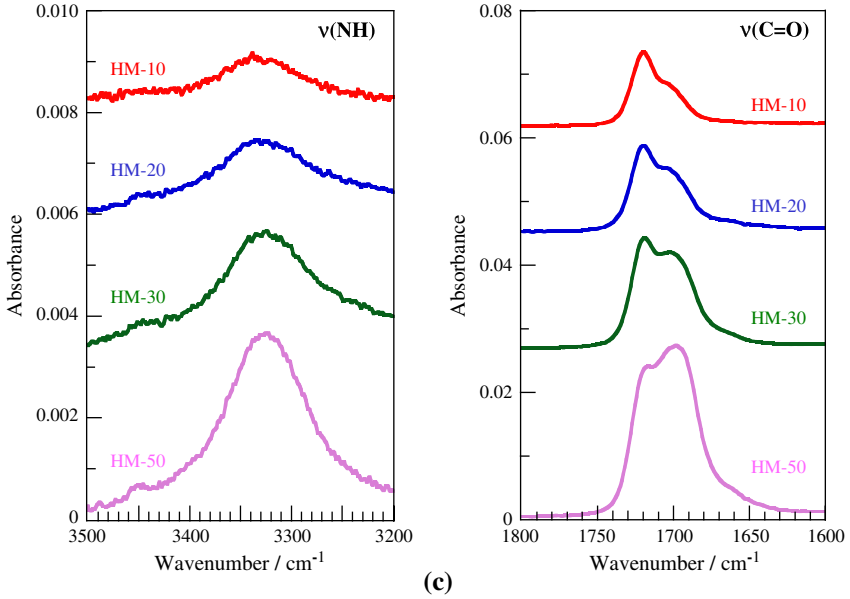

Fig. 4. Continued.

PUEs. $T_{g,s}$ of the NB- and IP-based PUEs clearly increased with increasing hard segment content. The increment of $T_{g,s}$ with increasing hard segment content for the NB-based PUE was smaller than that of IP one. In contrast, $T_{g,s}$ of the HM-based PUE increased only from −69.6 upto −68.5 °C and was almost independent on the hard segment content. $T_{g,s}$ of the HD-based PUE showed similar trend. It seems reasonable to conclude qualitatively from the results mentioned above that the order of degree of microphase separation of the PUEs is HD−PUE ≫ HM−PUE > IP PUE = NB−PUE.

Fig. 8 shows the WAXD profiles for the NB-, IP-, HM- and HD-based PUEs with 50 wt% hard segment content. The WAXD profiles of the NB-50 and IP-50 PUEs showed only amorphous halo at about 19°, in contrast, those of the HM-50 and HD-50 PUEs exhibited crystalline peaks as well as amorphous halo. These peak positions correspond well to those for the −(HM−BD)$_n$− and −(HD−BD)$_n$− of the hard segment model polyurethanes shown in Fig. 3. Therefore, the hard segment chains in the HM-50 and HD-50 PUEs crystallized and form the hard segment domains in the PUEs.

3.3. Mechanical properties of polyurethane elastomers

Since the PUEs with low hard segment content did show the plastic deformation, we compare the mechanical properties among four PUEs with 50 wt% hard segment content. Table 1 shows gel fraction, degree of swelling and mechanical properties of the NB-, IP-, HM- and HD-based PUEs. Degree of swelling with benzene for the NB-50, IP-50 and HM-50 PUEs was much greater than for the HD-50 and the order

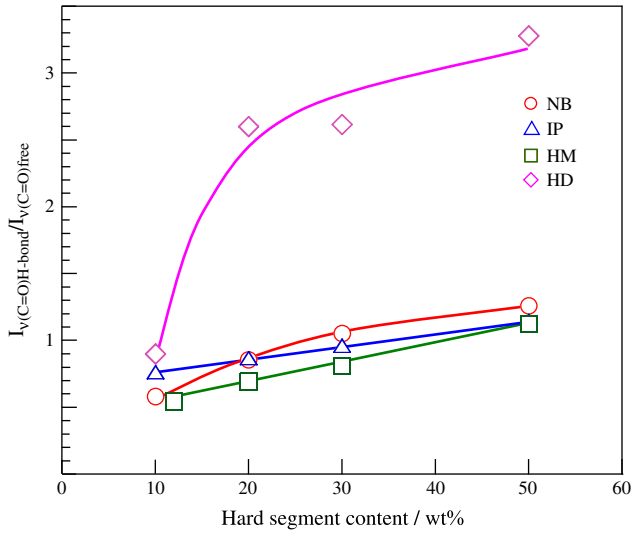

Fig. 5. Dependence on contents of hard segment of ratio of $\nu(C{=}O)_{H\text{-}bond}$ peak, to $\nu(C{=}O)_{free}$ ($\nu(C{=}O)_{H\text{-}bond}/\nu(C{=}O)_{free}$) for NB-, IP-, HM- and HD-based PUEs.

was IP- > NB- > HM- > HD-based PUEs. This can be explained well with the degree of microphase separation stated in previous section.

Fig. 9 shows the temperature dependence of the dynamic viscoelastic properties of the NB-50, IP-50, HM-50 and HD-50 PUEs. Two peaks at around −70 and 50 °C in tan δ curves correspond to α relaxation from soft segment phases. One is composed of soft segment rich phase and another includes a lot of hard segment components. For the cycloaliphatic diisocyanate-based PUEs, that is, the NB-, IP- and HM-based PUEs, the intensities of tan δ at higher temperature side (50 °C) were stronger in comparison with that of the HD-50. Rubbery plateau region in the dynamic storage modulus (E') for the NB-50 and IP-50 was observed above 60 °C, while that of the HM-50 was observed above 90 °C. The terminal temperature of rubbery plateau region of the NB-50 was higher than those of the IP-50 and HM-50 PUEs. This might be because the stiffness of the hard segment chains of the NB-based PUEs is

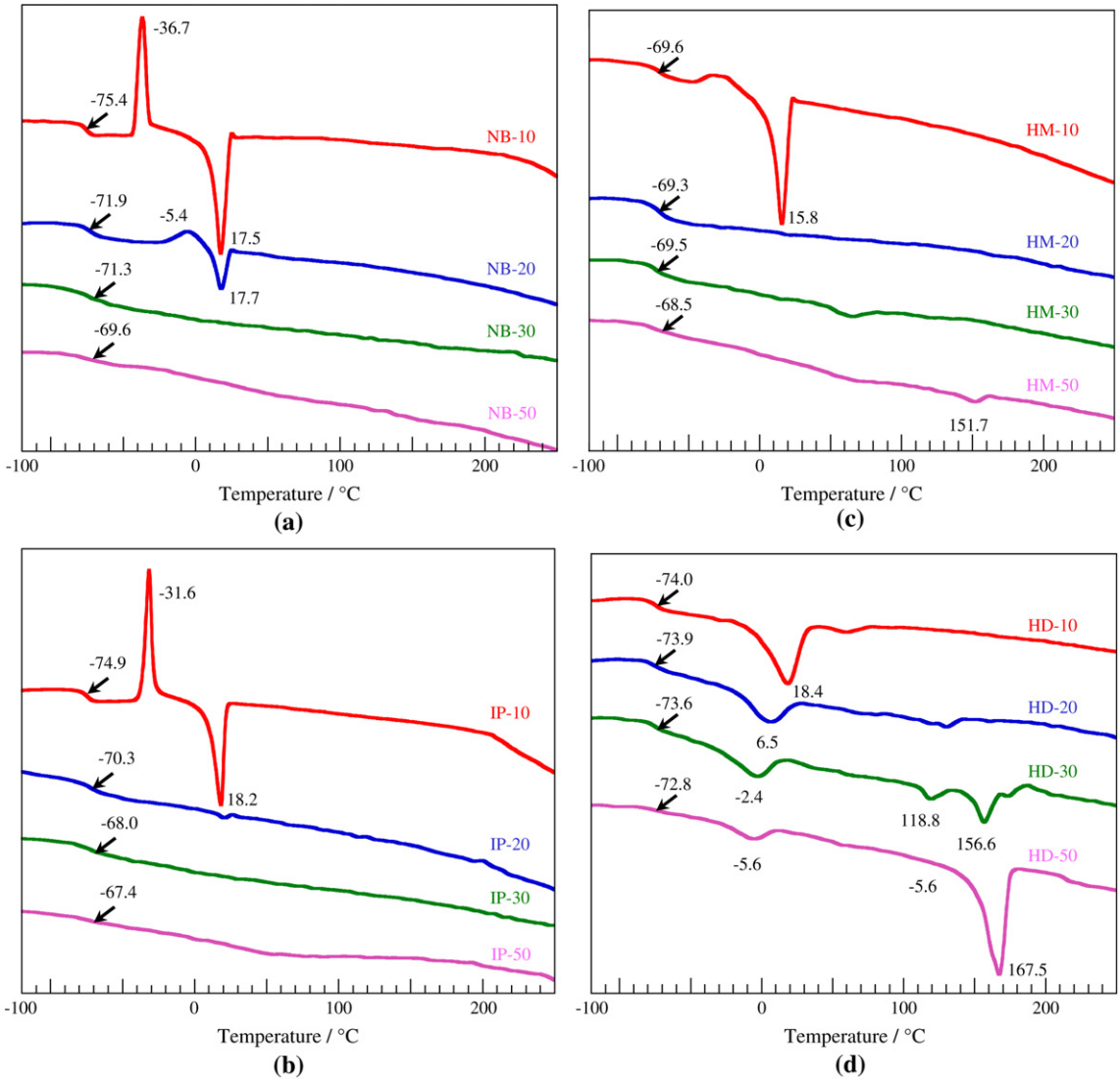

Fig. 6. DSC thermograms of (a) NB-, (b) IP-, (c) HM- and (d) HD-based PUEs with hard segment content from 10 to 50 wt%.

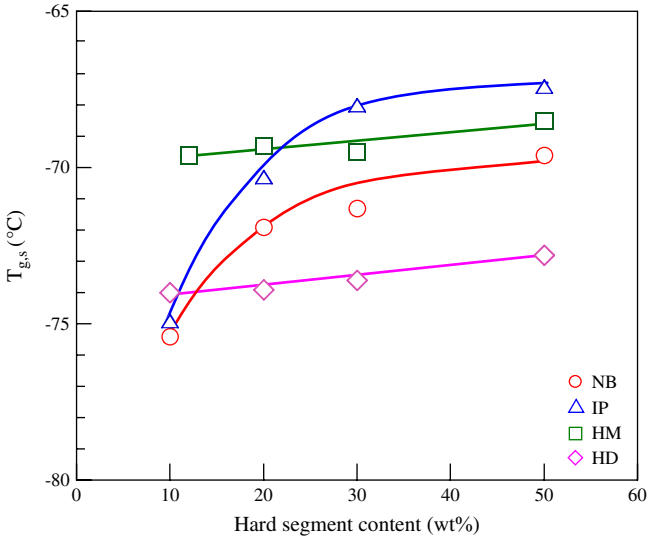

Fig. 7. Hard segment content dependence of $T_{g,s}$ for NB-, IP-, HM- and HD-based PUEs.

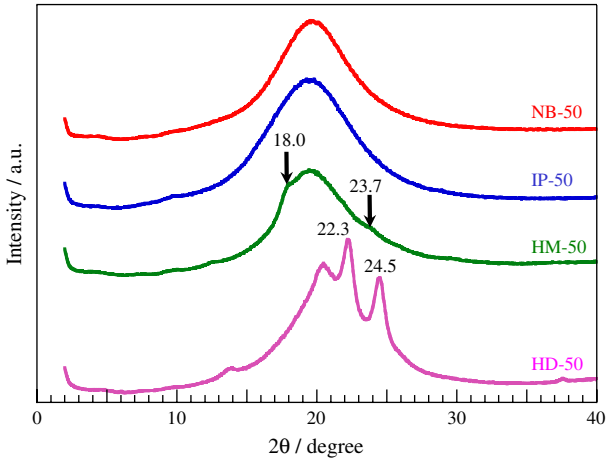

Fig. 8. WAXD profiles for the NB-, IP-, HM- and HD-based PUEs with 50 wt% hard segment content.

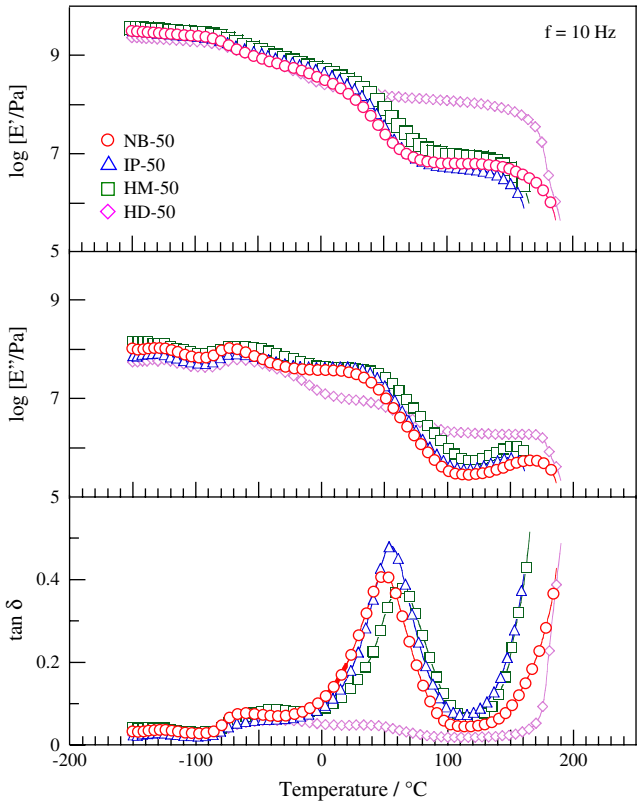

Fig. 9. Temperature dependence of dynamic storage modulus (E'), loss modulus (E'') and loss tangent (tan δ) of the NB-, IP-, HM- and HD-based PUEs with 50 wt% hard segment content.

higher than the IP- and HM-based PUEs. Also, E' of the rubbery plateau for the NB-50 PUEs was larger and smaller than those of the IP-50 and HM-50 PUEs, respectively, which corresponds well to the magnitude of Young's moduli. On the other hand, intensity of tan δ for the HD-50 was lower than other PUEs over the measured temperature. The intensity of tan δ for lower temperature side (−70 °C) is stronger than higher one, since the degree of microphase separation of the HD-50 is remarkably strong as shown in previous section. The HD-50 PUE showed rubbery plateau region at around 0 °C and very high E'. This is because HD-50 possesses the strong microphase separation and well-crystallized hard segment domains. This is easily expected from the fact that terminal temperature of the HD-50 was near its melting point of the hard segment.

Fig. 10 shows the stress–strain curves for the NB-50, IP-50, HM-50, and HD-50 PUEs measured at 20 °C. Young's moduli of four PUEs decreased in the following order: HD- > HM- > IPDI- = NB–PUEs. This is in a good agreement to that of the microphase-separated structure of the PUEs. That is, the NB-50 and IP-50 possess low Young's moduli because of insufficient organized hard segment domains. Young's modulus of the HM-50 exhibited middle position among four PUEs, because its cohesion force is not so strong because of lacking hydrogen bond among chains although the

Table 1
Gel fraction, degree of swelling and mechanical properties of NB-50, IP-50, HM-50 and HD-50 PUEs

Sample	Hardness [JIS-A]	Young's modulus [JIS-A]	Tensile strength [MPa]	Strain at break	Gel fraction [%]		Degree of swelling	
					Benzene	DMA	Benzene	DMA
NB-50	86	7.0	28.4	3.8	77	Soluble	6.89	Soluble
IP-50	88	7.8	26.0	3.3	95	Soluble	8.99	Soluble
HM-50	98	16.4	24.4	2.5	80	Soluble	5.27	Soluble
HD-50	100	21.9	41.8	4.2	91	Soluble	1.43	Soluble

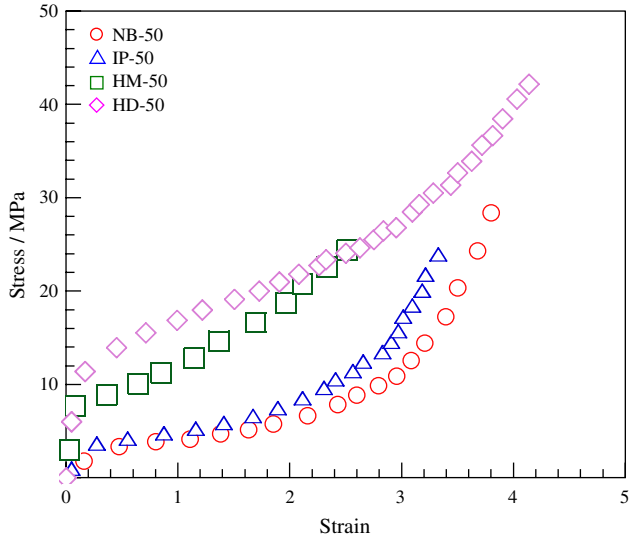

Fig. 10. Stress–strain curves for the NB-, IP-, HM- and HD-based PUEs with 50 wt% hard segment content measured at 20 °C.

hard segment chains are crystallizable. The HD-50 has strong microphase separation and highly-crystallized hard segment domains with hydrogen bonds, resulting that HD-50 PUE exhibited the largest tensile strength among four PUEs.

4. Conclusions

Microphase-separated structure and mechanical properties of the NB-based PUEs were studied and compared with those of cycloaliphatic diisocyanates-based (IP and HM) and aliphatic diisocyanate-based (HD) PUEs. Regular polyurethane of $-(NB-BD)_n-$ as a hard segment model was in the amorphous state same as $-(IP-BD)_n-$, in contrast, that for $-(HM-BD)_n-$ and $-(HD-BD)_n-$ were crystalline. Especially, hydrogen bonds among $-(HD-BD)_n-$ chains were quite progressed in comparison with other three models. For the PUEs, the NB- and IP-based PUEs had an inclination to phase mixing, leading to decreasing Young's modulus and tensile strength. The NB-based PUE has better heat resistance than the IP- and HM-based PUEs due to stiffness of NBDI backbone. The HM-based PUE has both properties of aliphatic and cycloaliphatic diisocyanates due to highly symmetrical structure compared with NB- and IP-based PUEs even if HMDI includes some isomers. The HD-based PUE exhibited high Young's modulus and tensile strength because of formation of hydrogen bonds and crystallization of the hard segment component and strong microphase separation.

References

[1] Petrovic ZS, Ferguson J. J Prog Polym Sci 1991;16:695.
[2] Ng HN, Allegrezza AE, Seymour RW, Cooper SL. Polymer 1972;14:255.
[3] Koberstein JT, Russell TP. Macromolecules 1986;19:714.
[4] Leung LM, Koberstein JT. J Polym Sci Polym Phys 1985;23:1883.
[5] Furukawa M, Komiya M, Yokoyama T. Angew Makromol Chem 1996;240:205.
[6] Furukawa M, Shiiba T, Murata S. Polymer 1999;40:1791.
[7] Martin DJ, Meijs GF, Renwick GM, Gunatillake PA, McCarthy SJ. J Appl Polym Sci 1996;60:557.
[8] Kojio K, Fukumaru T, Furukawa M. Macromolecules 2004;37:3287.
[9] Kojio K, Nonaka Y, Masubuchi T, Furukawa M. J Polym Sci Polym Phys Ed 2004;42:4448.
[10] Kojio K, Nakamura S, Furukawa M. Polymer 2004;45:8147.
[11] Schellenberger CS, Stewart FD. Adv Urethane Sci Technol 1975;4:68.
[12] Gardette JL, Lemaire J. Polym Degrad Stab 1984;6:135.
[13] Gerlock JL, Mielewski DF. Polym Degrad Stab 1989;23:41.
[14] NBDI™ Technical literature. Japan: Mitsui Takeda Chemicals, Inc.; 1997.
[15] Feiring AE, Crawford MK. J Fluorine Chem 2003;122:11.
[16] Kubota S. Kobunshi Ronbunshu 1996;53:465.
[17] Inoue S, Kondo M, Nakakita S, Shirasaka H, Okamoto H. Nihon Gomu Kyokaishi 2002;75:65.
[18] Saito Y, Nansai S, Kinoshita S. Polym J 1972;3:113.
[19] Lee HS, Wang YK, Hsu SL. Macromolecules 1987;20:2089.
[20] Brunette CM, Hsu SL, MacKnight WJ. Macromolecules 1982;15:71.